Control Engineering Practice 115 (2021) 104907

Contents lists available at ScienceDirect

Control Engineering Practice

journal homepage: www.elsevier.com/locate/conengprac

Event-triggered active disturbance rejection control for a class of networked systems with unmatched uncertainties: Theoretic and experimental results ☆

Kaixin Cui [a], Shu-Xia Tang [b], Yuan Huang [c], Hao Yu [d], Dawei Shi [a,*]

[a] State Key Laboratory of Intelligent Control and Decision of Complex Systems, School of Automation, Beijing Institute of Technology, Beijing, China
[b] Department of Mechanical Engineering, Texas Tech University, Lubbock, TX, USA
[c] Beijing Institute of Control Engineering, Beijing, China
[d] Department of Electrical and Computer Engineering, University of Alberta, Edmonton, AB, Canada

ARTICLE INFO

Keywords:
Event-triggered control
Networked system
Active disturbance rejection control
Unmatched uncertainty
Backstepping

ABSTRACT

In this work, an event-triggered control problem for a class of networked systems with unmatched uncertainties is investigated based on an active disturbance rejection control approach. To estimate the effect of unmatched uncertainties, a bank of extended state observers with guaranteed convergence is proposed. Based on the obtained estimates, a tracking-differentiator-enabled Zeno-free event-triggering condition is introduced with reduced sampling cost. An event-triggered controller is then designed to guarantee the closed-loop stability of the networked system with unmatched uncertainties, leveraging a backstepping control approach. Implementation issues of the proposed approach are discussed, and the effectiveness of the results is illustrated through experimental results on a DC torque motor platform.

1. Introduction

Networked control systems (NCSs) are highly reliable control systems in which the components exchange data through communication networks (Kim, Choi, & Mohapatra, 2009) and have been applied in a wide range of applications (Li, Zhang, & Li, 2014; Liang, Ge, Liu, Ling, & Liu, 2021; Wu & Xie, 2019). However, the performance of NCSs is restricted by energy constraints and the bandwidth limitations of communication channels (He, Hu, Xue, & Fang, 2017; Wang, Postoyan, Nešić, & Heemels, 2020). With the capability of reducing the communication rate, event-triggered data transmission protocols are adopted to transmit measurement updates only when the event-triggering conditions are violated (Liu, Wang, Wang, & Shi, 2020; Lu, Wu, Chen, & Cao, 2021; Trimpe & D'Andrea, 2014a).

The scope of this work belongs to event-triggered control of networked systems. A number of interesting attempts were devoted to obtaining efficient event-triggered control approaches. For instance, Åarzén (1999) proposed an event-based heuristic PID controller to obtain large reductions in central processing unit utilization. Tabuada (2007) investigated an event-triggered scheduler to solve stabilizing control problems on embedded processors. In Forni, Galeani, Nesic, and Zaccarian (2014), an event-triggered transmission policy was derived to reduce communication cost while preserving the closed-loop stability. An event-triggering condition based on the estimation variance was obtained in Trimpe and D'Andrea (2014b). Han et al. (2015) proposed an open-loop and a closed-loop stochastic event-triggered sensor schedule for the remote state estimation. Shi, Chen, and Darouach (2016) obtained that the closed-loop matrix of the optimal event-based estimator was exponentially stable for the time-varying case. In Brunner, Heemels, and Allgöwer (2019), an event-triggered and self-triggered controller was presented for linear systems based on reachable sets. Postoyan, Sanfelice, and Heemels (2019) analyzed the properties of the inter-event time for planar linear time-invariant systems controlled by an event-triggered state-feedback law. Liu, Li, and Shi (2020) leveraged the linearized augmented Lagrangian method to design an event-triggered decentralized algorithm, which addressed the decentralized optimization problem. In Liu, Li, Shi, and Xu (2020a), a dynamic event trigger that allowed the robust model predictive controller to solve the optimization problem only at triggering time instants was developed. For further results on event-triggered control, the interested authors can refer to Borgers, Dolk, and Heemels (2018), Kung, Wang, Wu, Shi, and Shi (2019), Liu, Li, Liu, and Tong (2021), Liu, Li, Shi, and Xu (2020b), Rathore, Fulwani, and Rathore (2020), Zhang, Ye, Chen, and Wang (2020) and references therein.

In this work, the stabilization problem for a class of networked systems with control-unmatched uncertainties is considered. Different

☆ This work was supported in part by the Beijing Natural Science Foundation, China under Grant 4192052 and in part by the National Natural Science Foundation of China under Grant 61973030.

* Corresponding author.
E-mail address: daweishi@bit.edu.cn (D. Shi).

https://doi.org/10.1016/j.conengprac.2021.104907
Received 5 June 2021; Received in revised form 15 July 2021; Accepted 17 July 2021
Available online xxxx
0967-0661/

from the event-triggered control for systems with full state information or matched uncertainties, the unmatched uncertainties of event-triggered systems are difficult to deal with and were not fully explored except for a few works. Sahoo, Xu, and Jagannathan (2013a) proposed an adaptive event-triggered controller using neural network approximation and feedback linearization for uncertain nonlinear systems, and Li and Yang (2018) investigated an event-triggered controller with online linear parameter estimators to stabilize the nonlinear system. In particular, the above approaches were designed using controllers with comprehensive structures, and it is yet to know whether it is possible to stabilize networked systems with unmatched uncertainties through an event-based controller with a simple structure, which motivates the investigation in this work.

Specifically, we focus on the event-based stabilization of a special class of networked systems for which each state is subject to control-unmatched uncertainties. To solve this problem, an active disturbance rejection control (ADRC) framework (Chen, Xue, & Huang, 2019; Madonski et al., 2020; Wei, Xue, & Li, 2019; Xue, Madonski, Lakomy, Gao, & Huang, 2017) is adopted and its main idea is to reject uncertainties actively such that the performance of the control system can be improved. ADRC was proved to be simple and effective in our earlier studies (Huang, Wang, Shi, & Shi, 2018; Huang, Wang, Shi, Wu, & Shi, 2019) and has been applied to various control problems (Li, Zhu, Mao, Su, & Li, 2021; Xue & Huang, 2014; Xue, Huang, & Gao, 2016). The key challenges of this work include how to estimate the effect of the unmatched uncertainties and how to ensure the stability of the event-triggered sampled-data system, while ensuring the implementability of the controller in practical engineering applications. The main results and contributions are summarized as follows:

1. A bank of extended state observers (ESOs) is designed to estimate the control-unmatched uncertainties. Under mild assumptions, we show that the asymptotic boundedness of the observation error can be guaranteed through Lyapunov analysis and comparison lemma (Theorem 1).
2. An event-triggered controller is developed to achieve closed-loop control at a reduced control update rate, which is made possible through designing a tracking-differentiator-enabled event-triggering mechanism. The Zeno-freeness of the proposed event-triggering condition is guaranteed, and the asymptotic stability of the event-triggered sampled-data system is proved by leveraging a backstepping technique (Theorem 2).
3. The effectiveness of the theoretic results is verified through experimental results on a DC torque motor system. We show that the proposed event-based controller can achieve satisfactory tracking performance for squarewave and sine-wave reference signals with reduced sampling cost.

The remainder of this work is organized as follows. After introducing the networked nonlinear systems with unmatched uncertainties, we present the problem formulation in Section 2. The theoretical results on the performance of the ESOs and the event-triggered backstepping controller is presented in Section 3 and Section 4. Finally, we verify the proposed controller through experiments on a DC motor system in Section 5, and summarize the conclusion and future work in Section 6.

2. Problem formulation

Consider the NCS scheme in Fig. 1. A networked nonlinear system with control-unmatched uncertainties is of the following form:

$$\begin{aligned}\dot{x}_i(t) &= x_{i+1}(t) + f_i(x_{1:i}(t), t), \quad i \in \{1, \dots, n-1\},\\ \dot{x}_n(t) &= u(t) + f_n(x_{1:n}(t), t),\end{aligned} \tag{1}$$

where $u(t) \in \mathbb{R}$ is the control input, $f(x(t), t) := f_{1:n}(x_{1:n}(t), t) \in \mathbb{R}^n$ denote the system uncertainties with $f_{1:i}(x_{1:i}(t), t) := [f_1(x_1(t), t), \dots, f_i(x_{1:i}(t), t)]^{\mathrm{T}} \in \mathbb{R}^i$ for $i \in \{1, \dots, n\}$, $x(t) := x_{1:n}(t) \in \mathbb{R}^n$ are the system states with $x_{1:i}(t) := [x_1(t), \dots, x_i(t)]^{\mathrm{T}} \in \mathbb{R}^i$ for $i \in \{1, \dots, n\}$. In this work, the order n of the system needs to be known. For the system in (1) we introduce the following assumptions.

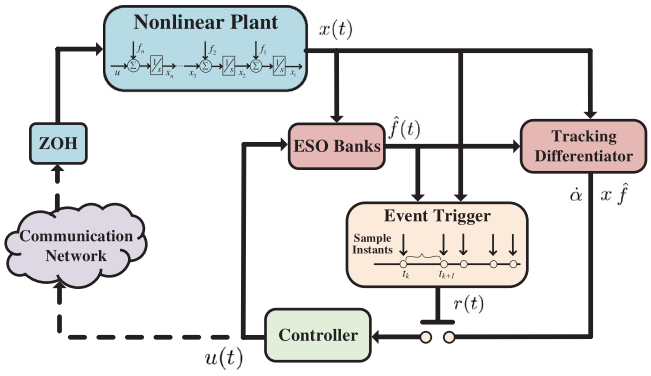

Fig. 1. Schematic of the proposed event-triggered control system.

Assumption 1. For any $i \in \{1, \dots, n\}$, the function $f_i(x_{1:i}, t) \in C^{n+1}(\mathbb{R}^i; \mathbb{R})$ satisfies:

$$\left|f_i(x_{1:i}, t)\right| \le c_{i0} + \sum_{j=1}^{i} c_{ij} \left|x_j\right|^{\kappa},$$

for some positive constants κ and c_{ij}, $j \in \{0, \dots, i\}$.

Assumption 2. For any $i \in \{1, \dots, n\}$, the system unknown uncertainty function $f_i(x_{1:i}, t)$ is continuous and satisfies the globally Lipschitz continuity:

$$\left|f_i(a_i, t_1) - f_i(b_i, t_2)\right| \le L_i \left\| [(a_i - b_i), (t_1 - t_2)] \right\|,$$

where a_i and b_i are vectors with appropriate dimensions, and L_i is a known constant.

Assumption 3. There exists a compact set $\mathcal{X}$ such that the solution $x_i(t)$ of system (1) is in the compact set:

$$|x_i(t)| \in \mathcal{X}, \quad i \in \{1, \dots, n\}, \ t \ge 0.$$

Note that Assumptions 1–3 are mild in general and have been widely adopted in existing investigations (Guo & Wu, 2017; Huang et al., 2018; Sahoo, Xu, & Jagannathan, 2013b; Zhao & Guo, 2015). In the engineering application of ADRC where the control scheme is "model-free", it is usually assumed that the process and disturbance are bounded but unknown. In particular, Assumptions 1 and 3 characterize the boundedness properties of the signals in a nonlinear system limited by operational and energy constraints; Assumption 1 indicates $\left|\frac{\partial f_i}{\partial t}\right| + \left\|\frac{\partial f_i}{\partial x_{1:i}}\right\| + \sum_{j=2}^{n}\left|f_i^{(j)}\right| \le c_{i0} + \sum_{j=1}^{i} c_{ij}\left|x_j\right|^{\kappa}$ where $f_i^{(j)}$ denotes the jth-order derivative of f_i, and Assumption 2 indicates the smoothness of the unknown nonlinear functions. Moreover, for systems have the same lower triangular structure, the boundedness of $\sum_{j=2}^{n}\left|f_i^{(j)}\right|$ can be ensured by designing an ESO with inverse state variables $\bar{x}_1 = x_1, \bar{x}_i = x_i + \sum_{j=1}^{i-1} f_{i-j}^{(j-1)}, i \in \{2, \dots, n\}$ (see Guo & Wu, 2017 for the technical details), which makes Assumption 1 more reasonable. In this work, we consider the scenario that the sensors and actuators of the controlled process are not closely installed; the controller needs to be implemented on either the sensor side or the actuator side and communication network is needed to achieve closed-loop control. To improve the utilization of communication resources, we aim to design a suitable backstepping controller together with a bank of ESOs and an event-triggering mechanism through addressing the following three questions:

1. How to design a bank of ESOs, the aim of which is to observe uncertainty functions and guarantee the observation performance?

2. How to propose a suitable event-triggering condition that can compromise the tradeoff between communication rate and system performance, and how to show there is no Zeno behavior?
3. How to design a backstepping controller that can maintain the stability of the system in (1)?

In addition, from an application perspective, the practical effectiveness of the proposed controller needs to be verified.

3. Extended state observer design

In this section, the problems stated above will be investigated in detail. As shown in Fig. 1, the basic idea is to first introduce a bank of ESOs to estimate the uncertainties $f(x(t),t)$, for which the estimates are expressed as $\hat{f}(t)$. Then, based on transmit measurement, an event-triggered controller is proposed through backstepping technique to stabilize the system (1). Note that only when the event is triggered, the measurement updates are transmitted. Thus, a zero-order holder (ZOH) module is utilized to retain the signals constant between two event instants. Firstly, we design a bank of ESOs to obtain uncertainty functions. One crucial idea of the extended state observer is to treat the uncertainty existed as an extended state. Thus, we define the extended state by

$$x_{n+i}(t) := f_i(x_{1:i}(t),t), \quad \forall\, i \in \{1,\dots,n\}.$$

Following the definition of the extended states, we expand the system (1) into a $2n$-dimensional form, based on which the ESOs are proposed as

$$\begin{aligned}
\dot{\hat{x}}_i(t) &= x_{i+1}(t) + \hat{x}_{n+i}(t) + g_i\Big(\sum_{j=1}^{i} q_j \frac{x_j(t)-\hat{x}_j(t)}{\varepsilon}\Big),\\
\dot{\hat{x}}_{n+i}(t) &= \frac{1}{\varepsilon} g_{n+i}\Big(\sum_{j=1}^{i} q_j \frac{x_j(t)-\hat{x}_j(t)}{\varepsilon}\Big),\ i \in \{1,\dots,n-1\},\\
\dot{\hat{x}}_n(t) &= u(t) + \hat{x}_{2n}(t) + g_n\Big(\sum_{j=1}^{n} q_j \frac{x_j(t)-\hat{x}_j(t)}{\varepsilon}\Big),\\
\dot{\hat{x}}_{2n}(t) &= \frac{1}{\varepsilon} g_{2n}\Big(\sum_{j=1}^{n} q_j \frac{x_j(t)-\hat{x}_j(t)}{\varepsilon}\Big),
\end{aligned} \tag{2}$$

where $\varepsilon \in (0,1)$ is the high-gain parameter, q_j's are adjustable parameters for $j \in \{1,\dots,i\}$ and $g_i(\cdot)$'s are continuous functions for $i \in \{1,\dots,n\}$ that can be designed to adjust the observation performance. Let $\hat{f}_i(t)$ denote the estimate of $f_i(t)$; in other words,

$$\hat{f}_i(t) := \hat{x}_{n+i}(t), \quad \forall\, i \in \{1,\dots,n\}.$$

Write $\hat{f}(t) := [\hat{f}_1(t),\dots,\hat{f}_n(t)]^{\mathrm{T}}$.

To better characterize the observation performance, we define the observation error variables $\tilde{x}_i(t)$ and $e_i(t)$ as

$$\tilde{x}_i(t) := x_i(t) - \hat{x}_i(t), \quad i \in \{1,\dots,2n\},$$

and

$$e_i(t) := \tilde{x}_i(t)/\varepsilon, \qquad i \in \{1,\dots,n\}, \tag{3a}$$

$$e_i(t) := \tilde{x}_i(t), \qquad i \in \{n+1,\dots,2n\}. \tag{3b}$$

Note that in the classical extended state observer scheme (Huang et al., 2019), only the control-matched uncertainty in nth dimensional dynamics is considered and there is only one extended state. However, since we consider the system with control-unmatched uncertainties in every dynamic channel in this work, we aim to design n extended states to observe the n terms of the control-unmatched uncertainties. Before continuing, the following assumption is made, which is a standard requirement in analyzing the asymptotic behavior of the ESO (Feng & Guo, 2017; Huang et al., 2018; Huang et al., 2019; Zhao & Guo, 2018).

Assumption 4. There exist positive constants β, λ_1, λ_2, λ_3, λ_4, adjustable parameters q_j's for $j \in \{1,\dots,i\}$, and continuously differentiable positive definite functions $V_i(\cdot) : \mathbb{R}^{2i} \to \mathbb{R}_0^+$ and $W_i(\cdot) : \mathbb{R}^{2i} \to \mathbb{R}_0^+$, $i \in \{1,\dots,n\}$, such that

1. $\lambda_1\|\omega\|^2 \le V_i(\omega) \le \lambda_2\|\omega\|^2$, $\lambda_3\|\omega\|^2 \le W_i(\omega) \le \lambda_4\|\omega\|^2$,
2. $\sum_{j=1}^{i}\big(\frac{\partial V_i}{\partial \omega_j}(\omega_{n+j} - g_j(q_1\omega_1 + \cdots + q_j\omega_j)) - \frac{\partial V_i}{\partial \omega_{n+j}}(g_{n+j}(q_1\omega_1 + \cdots + q_j\omega_j))\big) \le -W_i(\omega)$,
3. $\|\frac{\partial V_i}{\partial \omega}\| \le \beta\|\omega\|$,

where $\omega = [\omega_1, \omega_{n+1}, \dots, \omega_i, \omega_{n+i}]^{\mathrm{T}} \in \mathbb{R}^{2i}$.

With this assumption, we investigate the asymptotic boundedness property of observation errors between uncertainties $f(x(t),t)$ and the observed uncertainties $\hat{f}(t)$, which is shown in the following theorem.

Theorem 1. *Consider the system (1) and the bank of ESOs (2). If Assumptions 1, 3 and 4 hold, there exists $E > 0$ such that $\forall\, i \in \{1,\dots,n\}$ the observation errors are bounded with*

$$\limsup_{t\to\infty} |f_i(x_{1:i}(t),t) - \hat{f}_i(t)| \le E\varepsilon. \tag{4}$$

Proof. From (1) and (2), we observe that

$$\dot{\hat{x}}_i(t) = \tilde{x}_{n+i}(t) - g_i\Big(\sum_{j=1}^{i} q_j \frac{x_j(t)-\hat{x}_j(t)}{\varepsilon}\Big), \tag{5}$$

$$\dot{\hat{x}}_{n+i}(t) = \frac{\mathrm{d}}{\mathrm{d}t} f_i(x_{1:i}(t),t) - \frac{1}{\varepsilon} g_{n+i}\Big(\sum_{j=1}^{i} q_j \frac{x_j(t)-\hat{x}_j(t)}{\varepsilon}\Big),$$

for any $i \in \{1,\dots,n\}$. For notational brevity, write

$$h_i(t) := \frac{\mathrm{d}}{\mathrm{d}t} f_i(x_{1:i}(t),t).$$

Based on (3a), (3b) and (5), we obtain

$$\begin{aligned}
\dot{e}_i(t) &= \frac{1}{\varepsilon} e_{n+i}(t) - \frac{1}{\varepsilon} g_i\Big(\sum_{j=1}^{i} q_j e_j(t)\Big),\\
\dot{e}_{n+i}(t) &= h_i(t) - \frac{1}{\varepsilon} g_{n+i}\Big(\sum_{j=1}^{i} q_j e_j(t)\Big).
\end{aligned}$$

Considering a positive semidefinite function $V_i(e^i(t))$, $i \in \{1,\dots,n\}$, we have

$$\begin{aligned}
\dot{V}_i(e^i(t)) = &\sum_{j=1}^{i}\Big(\frac{1}{\varepsilon}\frac{\partial V_i}{\partial e_j(t)}(e_{n+j}(t) - g_j(q_1e_1(t) + \cdots + q_je_j(t)))\\
&- \frac{1}{\varepsilon}\frac{\partial V_i}{\partial e_{n+j}(t)}(g_{n+j}(q_1e_1(t) + \cdots + q_je_j(t))) + \frac{\partial V_i}{\partial e_{n+j}(t)} h_j(t)\Big),
\end{aligned}$$

with $e^i(t) := [e_1(t), e_{n+1}(t), \dots, e_i(t), e_{n+i}(t)]^{\mathrm{T}} \in \mathbb{R}^{2i}$. From Assumption 1, there exists $M > 0$ such that we have $|h_i(t)| < M$. With items (2) and (3) in Assumption 4, we obtain an upper bound for the dynamics of $V_i(e^i(t))$ as

$$\begin{aligned}
\dot{V}_i(e^i(t)) &\le -\frac{1}{\varepsilon} W_i(e^i(t)) + \beta i M\|e^i(t)\|\\
&\le -\frac{\lambda_3}{\lambda_2\varepsilon} V_i(e^i(t)) + \frac{\sqrt{\lambda_1}}{\lambda_1}\beta i M\sqrt{V_i(e^i(t))}.
\end{aligned} \tag{6}$$

Let $Q_i(e^i(t)) := \sqrt{V_i(e^i(t))}$. Therefore,

$$\dot{V}_i(e^i(t)) = 2Q_i(e^i(t))\dot{Q}_i(e^i(t)), \tag{7}$$

$$\sqrt{\lambda_1}\|e^i(t)\| \le Q_i(e^i(t)) \le \sqrt{\lambda_2}\|e^i(t)\|. \tag{8}$$

We further have a linear differential inequality

$$\dot{Q}_i(e^i(t)) \le -\frac{\lambda_3}{2\lambda_2\varepsilon} Q_i(e^i(t)) + \frac{\beta i M\sqrt{\lambda_1}}{2\lambda_1}, \tag{9}$$

when $Q > 0$. From item (1) in Assumption 4, we obtain that $\lambda_1\|e^i\|^2 \le V_i(e^i) \le \frac{\beta}{2}\|e^i\|^2$, which means $\beta \ge 2\lambda_1$. For $Q = 0$, we have

$$D^+Q_i(e^i(t)) \le \frac{\beta i M\sqrt{\lambda_1}}{2\lambda_1},$$

where $D^+Q_i(e^i(t))$ denotes the upper right-hand derivative of $Q_i(e^i(t))$; thus $D^+Q_i(e^i(t))$ satisfies (9) for all $V_i(e^i(t)) \ge 0$. From the comparison lemma provided in Khalil (2002) and combining the above results on (9), for any $i \in \{1,\dots,n\}$, we obtain

$$\begin{aligned} Q_i(e^i(t)) \le \exp\Big(-\frac{\lambda_3}{2\lambda_2\varepsilon}(t-t_0)\Big)Q_i(e^i(t_0)) \\ + \frac{\beta i M\sqrt{\lambda_1}}{2\lambda_1}\int_{t_0}^{t}\exp\Big(-\frac{\lambda_3}{2\lambda_2\varepsilon}(t-\tau)\Big)d\tau. \end{aligned} \tag{10}$$

From (8) and (10), we have

$$\begin{aligned} \|e^i(t)\| \le \sqrt{\frac{\lambda_2}{\lambda_1}}\|e^i(t_0)\|\exp\Big(-\frac{\lambda_3}{2\lambda_2\varepsilon}(t-t_0)\Big) \\ + \Big(1-\exp\Big(-\frac{\lambda_3}{2\lambda_2\varepsilon}(t-t_0)\Big)\Big)\frac{\beta i\lambda_2 M\varepsilon}{\lambda_1\lambda_3}. \end{aligned} \tag{11}$$

For notational brevity, we define the right side of the inequality (11) as $m(t)$. Specifically, when $t \to \infty$, we obtain

$$\exp\Big(-\frac{\lambda_3}{2\lambda_2\varepsilon}(t-t_0)\Big) \to 0.$$

Namely we have $m(t) \to \frac{\beta i\lambda_2 M\varepsilon}{\lambda_1\lambda_3}$ when $t \to \infty$, which indicates

$$\|e^i(t)\| \le \frac{\beta i\lambda_2 M\varepsilon}{\lambda_1\lambda_3}.$$

Based on (2)–(3b), it follows that $|e_{n+i}(t)| = |x_{n+i}(t) - \hat{x}_{n+i}(t)| = |f_i(x_{1:i}(t),t) - \hat{f}_i(t)|$, for any $i \in \{1,\dots,n\}$. Thus, we have

$$|f_i(x_{1:i}(t),t) - \hat{f}_i(t)| \le m(t). \tag{12}$$

If we define $E := \frac{\beta i\lambda_2 M}{\lambda_1\lambda_3} > 0$ with positive constants β, λ_1, λ_2, λ_3 and M, we directly obtain that

$$\limsup_{t\to\infty}|f_i(x_{1:i}(t),t) - \hat{f}_i(t)| \le E\varepsilon, \tag{13}$$

with $1 \le i \le n$, which completes the proof. ■

Remark 1. For the bank of ESOs, functions $g_i(\cdot)$'s can be linear or non-linear as long as Assumption 4 is satisfied; in particular, the case of linear $g_i(\cdot)$'s is naturally covered by Assumption 4 as a special case (see Section 5 for an example that adopts a linear ESO bank). In this work, the weighting parameters q_j's are adjustable to make explicit use of the measured state signals. Specifically, setting $q_j = 1$ for $j = i$ and $q_j = 0$ for $j \ne i$ in $g_i(\cdot)$, $g_i\Big(\sum_{j=1}^{i} q_j\frac{x_j(t)-\hat{x}_j(t)}{\varepsilon}\Big)$ reduces to $g_i(x_i(t)-\hat{x}_i(t))/\varepsilon$, which is utilized in Wu, Deng, Guo, and Xiang (2021).

Remark 2. In general, the estimation errors are evaluated by both the steady and transient performance. Similar to Xue and Huang (2014) and Zhao and Guo (2015), the transient performance of the estimation error can also be concluded in this work. Specifically, from (11), there exists an $\varepsilon^* > 0$, such that for any $T > 0$ and any $\varepsilon \in (0,\varepsilon^*)$, it holds that $\|e^i(t)\| \le O(\varepsilon,t)$ uniformly in $t \in [T,\infty)$, where $O(\varepsilon,t)$ is designed as $O(\varepsilon,t) := \sqrt{\frac{\lambda_2}{\lambda_1}}\|e^i(t_0)\|\exp\Big(-\frac{\lambda_3}{2\lambda_2\varepsilon}(t-t_0)\Big) + \Big(1-\exp\Big(-\frac{\lambda_3}{2\lambda_2\varepsilon}(t-t_0)\Big)\Big)\frac{\beta i\lambda_2 M\varepsilon}{\lambda_1\lambda_3}$. The upper bound $O(\varepsilon,t)$ is an ε-dependent and time-dependent variable. Thus, we can obtain an upper bound of the estimation error at any time t to quantify the transient performance.

Remark 3. In this remark, we briefly analyze the effect of measurement noise on ESO estimation performance. Since the real state variable $x_i(t)$ becomes unknown in the existence of measurement noise, we can only obtain the noisy measurements of the states, which are defined by $\xi_i(t)$ for $i \in \{1,\dots,n\}$. In this scenario, the ESOs are reformulated as

$$\begin{aligned} \dot{\hat{x}}_i(t) &= \xi_{i+1}(t) + \hat{x}_{n+i}(t) + g_i\Big(\sum_{j=1}^{i} q_j\frac{\xi_j(t)-\hat{x}_j(t)}{\varepsilon}\Big), \\ \dot{\hat{x}}_{n+i}(t) &= \frac{1}{\varepsilon}g_{n+i}\Big(\sum_{j=1}^{i} q_j\frac{\xi_j(t)-\hat{x}_j(t)}{\varepsilon}\Big),\ i \in \{1,\dots,n-1\}, \\ \dot{\hat{x}}_n(t) &= u(t) + \hat{x}_{2n}(t) + g_n\Big(\sum_{j=1}^{n} q_j\frac{\xi_j(t)-\hat{x}_j(t)}{\varepsilon}\Big), \\ \dot{\hat{x}}_{2n}(t) &= \frac{1}{\varepsilon}g_{2n}\Big(\sum_{j=1}^{n} q_j\frac{\xi_j(t)-\hat{x}_j(t)}{\varepsilon}\Big). \end{aligned}$$

Define the measurement error $\eta_i(t)$ and a new variable $s_i(t)$ as $\eta_i(t) := (\xi_i(t) - x_i(t))/\varepsilon$, $s_i(t) := g_i(\sum_{j=1}^{i} q_j e_j(t) + \sum_{j=1}^{i} q_j\eta_j(t)) - g_i(\sum_{j=1}^{i} q_j e_j(t))$ and $s_{n+i}(t) := g_{n+i}(\sum_{j=1}^{i} q_j e_j(t) + \sum_{j=1}^{i} q_j\eta_j(t)) - g_i(\sum_{j=1}^{i} q_j e_j(t))$ for $i \in \{1,\dots,n\}$, respectively. If function $g_i(\cdot)$ is designed Lipschitz with $l_i > 0$, we can obtain $|s_i(t)| := |g_i(\sum_{j=1}^{i} q_j e_j(t) + \sum_{j=1}^{i} q_j\eta_j(t)) - g_i(\sum_{j=1}^{i} q_j e_j(t))| \le l_i|\sum_{j=1}^{i} q_j\eta_j(t)|$ and $|s_{n+i}(t)| := |g_{n+i}(\sum_{j=1}^{i} q_j e_j(t) + \sum_{j=1}^{i} q_j\eta_j(t)) - g_i(\sum_{j=1}^{i} q_j e_j(t))| \le l_{n+i}|\sum_{j=1}^{i} q_j\eta_j(t)|$ for $i \in \{1,\dots,n\}$. The observation error $e_i(t)$ becomes

$$\begin{aligned} \dot{e}_i(t) &= -\eta_{i+1}(t) + \frac{1}{\varepsilon}e_{n+i}(t) - \frac{1}{\varepsilon}g_i\Big(\sum_{j=1}^{i} q_j e_j(t)\Big) - \frac{1}{\varepsilon}s_i(t), \\ \dot{e}_{n+i}(t) &= h_i(t) - \frac{1}{\varepsilon}g_{n+i}\Big(\sum_{j=1}^{i} q_j e_j(t)\Big) - \frac{1}{\varepsilon}s_{n+i}(t). \end{aligned}$$

Then, we have $\dot{V}_i(e(t)) \le -\frac{\lambda_3}{\lambda_2\varepsilon}V_i(e(t)) + \frac{\sqrt{\lambda_1}}{\lambda_1}\beta i M\sqrt{V_i(e(t))} + \frac{\beta\sqrt{\lambda_1}}{\lambda_1}\sum_{j=1}^{i}|\eta_{i+1}(t)|\sqrt{V_i(e(t))} + \frac{\beta\sqrt{\lambda_1}}{\varepsilon\lambda_1}\sum_{j=1}^{i}|s_j(t)+s_{n+j}(t)|\sqrt{V_i(e(t))}$. Following a similar line of arguments as the proof of Theorem 1, we can also obtain an upper bound of the observation error:

$$\begin{aligned} \limsup_{t\to\infty}|f_i(x_{1:i}(t),t) - \hat{f}_i(t)| \le E\varepsilon + \frac{\lambda_2\beta}{\lambda_1\lambda_3}\sup_{t>0}\sum_{j=1}^{i}|\xi_{j+1}(t) - x_{j+1}(t)| \\ + \frac{\lambda_2\beta}{\lambda_1\lambda_3}\sup_{t>0}\sum_{j=1}^{i}(l_j + l_{n+j})\Big|\sum_{J=1}^{j} q_J\frac{\xi_J(t)-x_J(t)}{\varepsilon}\Big|. \end{aligned}$$

From the above expression, the measurement noise could be amplified to $\eta_i(t)$ by the high-gain parameter ε, which indicates that given the range of measurement errors, an appropriate ε needs to be carefully designed to maintain observation performance.

Remark 4. Note that a time-varying choice of the high-gain parameter can also be adopted in the proposed ESO design, to mitigate the peaking value problem in the initial stage caused by the difference between the initial states of the system and the ESO bank (Zhao & Guo, 2015). For instance, define

$$\psi(t) := \begin{cases} e^{at}, & 0 \le t < \ln(1/\varepsilon)/a, \\ 1/\varepsilon, & t \ge \ln(1/\varepsilon)/a, \end{cases} \tag{14}$$

where a is a positive constant. An ESO bank with a time-varying gain parameter of the following form can be considered:

$$\begin{aligned} \dot{\hat{x}}_i(t) &= x_{i+1}(t) + \hat{x}_{n+i}(t) + g_i\Big(\sum_{j=1}^{i}\psi(t)\big(q_j(x_j(t)-\hat{x}_j(t))\big)\Big), \\ \dot{\hat{x}}_{n+i}(t) &= \psi(t)g_{n+i}\Big(\sum_{j=1}^{i}\psi(t)\big(q_j(x_j(t)-\hat{x}_j(t))\big)\Big), \\ \dot{\hat{x}}_n(t) &= u(t) + \hat{x}_{2n}(t) + g_n\Big(\sum_{j=1}^{n}\psi(t)\big(q_j(x_j(t)-\hat{x}_j(t))\big)\Big), \\ \dot{\hat{x}}_{2n}(t) &= \psi(t)g_{2n}\Big(\sum_{j=1}^{n}\psi(t)\big(q_j(x_j(t)-\hat{x}_j(t))\big)\Big), \end{aligned} \tag{15}$$

with $i \in \{1, \dots, n-1\}$. Following a similar line of arguments as the proof of Theorem 1, we can also obtain a bound on the observation error

$$\limsup_{t\to\infty} |f_i(x_{1:i}(t), t) - \hat{f}_i(t)| \le E\varepsilon.$$

The key intuition is that due to the fact that when $t \ge \ln(1/\varepsilon)/a$, the ESO with a time-varying gain in (15) reduce to the ESO in (2).

4. Controller design

The above results reveal that the estimation error between the uncertainty function $f_i(x_{1:i}(t), t)$ and the observed uncertainty $\hat{f}_i(t)$ is guaranteed to be bounded by suitably designing the high-gain parameter ε and the observer function $g_i(\cdot)$. Next, we utilize the obtained $\hat{f}_i(t)$ to build an event-based controller through a backstepping control technique. Firstly, define

$$\begin{aligned} z_1(t) &:= x_1(t), \\ z_i(t) &:= x_i(t) - \alpha_{i-1}(t), \quad 1 < i \le n, \end{aligned} \tag{16}$$

where $x_i(t)$ is the system state and $\alpha_{i-1}(t)$ is the virtual input function designed at $i-1$ step:

$$\begin{aligned} \alpha_1(t) &:= -k_1 z_1(t) - \hat{f}_1(t), \\ \alpha_i(t) &:= -z_{i-1}(t) - k_i z_i(t) - \hat{f}_i(t) + \dot{\alpha}_{i-1}(t), \end{aligned} \tag{17}$$

with $k_i > 1/2$ and $i \in \{2, \dots, n-1\}$.

To obtain the differential of virtual input $\alpha_i(t)$ with $i \in \{1, \dots, n-1\}$, we adopt the following tracking differentiator,

$$\dot{\tilde{\alpha}}_i(t) = R^2\Big(a_1(\tilde{\alpha}_i(t) - \alpha_i(t)) + \frac{a_2 \dot{\tilde{\alpha}}_i(t)}{R}\Big), \tag{18}$$

where $\tilde{\alpha}_i(t)$ is the estimate of $\alpha_i(t)$, and R, a_1 and a_2 are designed parameters. We can obtain the bounded tracking performance when signals $\alpha_i(t)$, $\dot{\alpha}_i(t)$ and $\ddot{\alpha}_i(t)$ are all bounded (Guo & Han, 2000; Guo & Zhao, 2011; Guo & Zhao, 2011). For the system considered, we observe from (17) that $\alpha_i(t)$ is a simple combination of $x_i(t)$ and $\hat{f}_i(t)$. Since $x(t)$, $\dot{x}(t)$, $\hat{f}_i(t)$ and $\dot{\hat{f}}_i(t)$ are bounded (*c.f.*, Eqs. (1), (2) and Assumption 3), $\alpha_i(t)$ and $\dot{\alpha}_i(t)$ are bounded, and $\ddot{\alpha}_i(t)$ is bounded since $g_i(\cdot)$ is designed as a continuous and differentiable function. Note that in Theorem 2.1 and Theorem 3.1 of Guo and Zhao (2011), only signals $\alpha_i(t)$ and $\dot{\alpha}_i(t)$ need to be bounded when $\dot{\alpha}_i(t)$ satisfies the locally Lipschitz continuous condition. In this work, however, $\dot{\alpha}_i(t)$ is not guaranteed to be a locally Lipschitz continuous function, which is why $\ddot{\alpha}_i(t)$ needs to be bounded as well. Then, from Theorem 3.2 in Guo and Zhao (2011), Guo and Zhao (2011), we have

$$\begin{aligned} \dot{\tilde{\alpha}}_i(t) - \dot{\alpha}_i(t) &= \left[(RA)e^{RAt}\right]_1 Y_R(0) \\ &+ \left[e^{ARt}\right]_{11} \dot{\alpha}_i(0) + \int_0^{Rt} \left[e^{A(Rt-s)}\right]_{11} \frac{\ddot{\alpha}_i\left(\frac{s}{R}\right)}{R} ds, \end{aligned} \tag{19}$$

where the matrix $A := \left[\begin{smallmatrix} 0 & 1 \\ a_1 & a_2 \end{smallmatrix}\right]$ is Hurwitz and $Y_R(0) := \left(\tilde{\alpha}_i(0) - \alpha_i(0), \frac{\dot{\tilde{\alpha}}_i(0)}{R}\right)^{\mathrm{T}}$. For notational brevity, let a new bounded variable $\theta_i(t)$ denote the tracking error between $\dot{\alpha}_i(t)$ and $\dot{\tilde{\alpha}}_i(t)$ with $i \in \{1, \dots, n-1\}$ as

$$\dot{\tilde{\alpha}}_i(t) - \dot{\alpha}_i(t) := \theta_i(t). \tag{20}$$

From Guo and Zhao (2011), $\theta(t) \to 0$ when $R \to \infty$, and we obtain that $\dot{\theta}_i(t)$ is bounded with $\dot{\theta}_i(t) = \dddot{\tilde{\alpha}}_i(t) - \dddot{\alpha}_i(t)$ from (18)–(20). In addition, we define $\hat{z}_i(t)$ as the estimate of $z_i(t)$ obtained by replacing $\alpha_i(t)$ in Eq. (16) with $\tilde{\alpha}_i(t)$, and define $o_i(t)$ as the error between $z_i(t)$ and $\hat{z}_i(t)$ for $i \in \{1, \dots, n\}$:

$$o_i(t) := z_i(t) - \hat{z}_i(t). \tag{21}$$

From (16), (17), (20) and (21), the following recursive expressions can be obtained

$$o_i(t) = o_{i-2}(t) + k_{i-1} o_{i-1}(t) + \theta_{i-2}(t), \tag{22}$$

and $\dot{o}_i(t) = \dot{o}_{i-2}(t) + k_{i-1}\dot{o}_{i-1}(t) + \dot{\theta}_{i-2}(t)$. Note that $\dot{o}_i(t)$ is bounded and when $R \to \infty$, we have $o_i(t) \to 0$.

With the estimated $\hat{z}_i(t)$, the control input $u(t)$ can be introduced that is only updated at the triggering instants t_k. Specifically, for $t \in [t_k, t_{k+1})$, $u(t)$ is considered as

$$u(t) := -\hat{z}_{n-1}(t_k) - k_n \hat{z}_n(t_k) - \hat{f}_n(t_k) + \dot{\tilde{\alpha}}_{n-1}(t_k), \tag{23}$$

where t_k denotes the previous event-triggering time instant and k denotes the total number of triggering events during the time period $[t_0, t)$. To design the event-triggering condition, we define two new variables:

$$\delta_i(t) := \hat{z}_i(t) - \hat{z}_i(t_k), \quad i \in \{1, \dots, n\}, \tag{24}$$

$$\sigma_i(t) := x_i(t) - x_i(t_k), \quad i \in \{1, \dots, n\}. \tag{25}$$

From the system (1), (16) and (17), the system dynamics can be reformulated as

$$\dot{z}_1(t) = z_2(t) - k_1 z_1(t) - \hat{f}_1(t) + f_1(x_1(t), t), \tag{26}$$

$$\begin{aligned} \dot{z}_i(t) &= z_{i+1}(t) - z_{i-1}(t) - k_i z_i(t) - \hat{f}_i(t) + f_i(x_{1:i}(t), t), \\ &\quad i \in \{2, \dots, n-1\}, \end{aligned} \tag{27}$$

$$\begin{aligned} \dot{z}_n(t) &= -\hat{z}_{n-1}(t_k) - k_n \hat{z}_n(t_k) - \hat{f}_n(t_k) \\ &\quad + \dot{\tilde{\alpha}}_{n-1}(t_k) - \dot{\alpha}_{n-1}(t) + f_n(x_{1:n}(t), t). \end{aligned} \tag{28}$$

According to (21) and (24), we obtain

$$z_i(t) - \hat{z}_i(t_k) = z_i(t) - \hat{z}_i(t) + \hat{z}_i(t) - \hat{z}_i(t_k) = o_i(t) + \delta_i(t).$$

Then, by adding and subtracting $\dot{\tilde{\alpha}}_{n-1}(t)$ and $f_n(x_{1:n}(t_k), t_k)$ to (28), we have

$$\begin{aligned} \dot{z}_n(t) &= -z_{n-1}(t) + o_{n-1}(t) + \delta_{n-1}(t) - k_n z_n(t) \\ &\quad + k_n o_n(t) + k_n \delta_n(t) + \dot{\tilde{\alpha}}_{n-1}(t_k) - \dot{\tilde{\alpha}}_{n-1}(t) \\ &\quad + \dot{\tilde{\alpha}}_{n-1}(t) - \dot{\alpha}_{n-1}(t) - \hat{f}_n(t_k) + f_n(x_{1:n}(t_k), t_k) \\ &\quad - f_n(x_{1:n}(t_k), t_k) + f_n(x_{1:n}(t), t). \end{aligned} \tag{29}$$

From the above equations, one way of ensuring the system performance is to design an event-triggering condition such that the sampled state errors and sampled tracking error are restricted to be less than the dynamic state in (29), which motivates the design of the following event-triggering condition:

$$r(t) := \begin{cases} 0, & \text{if } |\delta_{n-1}(t)| + k_n|\delta_n(t)| + L_n\|\sigma_{1:n}(t)\| \\ & \quad + L_n|t - t_k| + |\dot{\tilde{\alpha}}_{n-1}(t_k) - \dot{\tilde{\alpha}}_{n-1}(t)| \\ & \quad \le \Gamma|\hat{z}_n(t)| + \epsilon, \\ 1, & \text{otherwise}, \end{cases} \tag{30}$$

where $\sigma_{1:n} := [\sigma_1, \dots, \sigma_n]^{\mathrm{T}}$, $L_n > 0$ is defined in Assumption 2, $\epsilon > 0$ and $\Gamma > 0$, satisfying $\Gamma < k_i - \frac{1}{2}$ for all $i \in \{1, \dots, n\}$, are user-specified constants. It is shown that the sampling instants are determined by the event-triggering condition. In other words, when $|\delta_{n-1}(t)| + k_n|\delta_n(t)| + L_n\|\sigma_{1:n}(t)\| + L_n|t - t_k| + |\dot{\tilde{\alpha}}_{n-1}(t_k) - \dot{\tilde{\alpha}}_{n-1}(t)| \le \Gamma|\hat{z}_n(t)| + \epsilon$ is violated, namely $r(t) = 1$, and the system measurement information is transmitted.

For the event-triggered control scheme introduced above, the following results can be obtained for the asymptotic behavior of the closed-loop system.

Theorem 2. *Consider the dynamical system (26), (27), (29), the virtual input functions (17), the event-triggering condition (30) and the control input law (23). Suppose Assumptions 1–4 hold. Then, there exist $D > 0$, $p > 0$ and $\tau > 0$, such that the system state $z_i(t)$ and the sampling interval $\{t_{k+1} - t_k\}$ for any $k \ge 0$ satisfy*

$$\limsup_{t\to\infty, R\to\infty} |z_i(t)| \le \sqrt{D/p},$$

$$\min\{t_{k+1} - t_k\} \ge \tau.$$

Proof. Define the Lyapunov function $V_z^\star(z(t))$ as

$$V_z^\star(z(t)) := \sum_{i=1}^{n} \frac{1}{2} z_i^2(t),$$

where $z := [z_1, \dots, z_n]^{\mathrm{T}}$. Recalling Eqs. (26), (27) and (29), the dynamics of $V_z^\star(z(t))$ is derived as

$$\begin{aligned}
\dot{V}_z^\star(z(t)) &= \textstyle\sum_{i=1}^{n} z_i(t)\dot{z}_i(t) = \big[z_1(t)(z_2(t) - k_1 z_1(t) \\
&- \hat{f}_1(t) + f_1(x_1(t), t))\big] + \textstyle\sum_{i=2}^{n-1}\big[z_i(t)(z_{i+1}(t) - z_{i-1}(t) \\
&- k_i z_i(t) - \hat{f}_i(t) + f_i(x_{1:i}(t), t))\big] + \big[z_n(t)(-z_{n-1}(t) \\
&+ o_{n-1}(t) + \delta_{n-1}(t) - k_n z_n(t) + k_n o_n(t) + k_n \delta_n(t) \\
&+ \dot{\tilde{\alpha}}_{n-1}(t_k) - \dot{\tilde{\alpha}}_{n-1}(t) + \dot{\tilde{\alpha}}_{n-1}(t) - \dot{\alpha}_{n-1}(t) - \hat{f}_n(t_k) \\
&+ f_n(x_{1:n}(t_k), t_k) - f_n(x_{1:n}(t_k), t_k) + f_n(x_{1:n}(t), t))\big].
\end{aligned}$$

Based on Assumption 2, it suffices to show $f_n(x_{1:n}(t), t) - f_n(x_{1:n}(t_k), t_k) \le L_n \big\|(x_{1:n}(t) - x_{1:n}(t_k)), (t - t_k)\big\| \le L_n \|\sigma_{1:n}\| + L_n|t - t_k|$. In addition, from (12), (20) and (21), we have

$$\begin{aligned}
\dot{V}_z^\star(z(t)) &\le \textstyle\sum_{i=1}^{n}\big[|z_i(t)|(-k_i|z_i(t)| + m(t))\big] + \big[\,|z_n(t)| \\
&(|o_{n-1}(t)| + |\delta_{n-1}(t)| + k_n|o_n(t)| + k_n|\delta_n(t)| + |\dot{\tilde{\alpha}}_{n-1}(t_k) \\
&- \dot{\tilde{\alpha}}_{n-1}(t)| + |\theta(t)| + L_n \,\|\, \sigma_{1:n}(t) \,\|\, + L_n|t - t_k|)\,\big]\,.
\end{aligned}$$

Recalling the event-triggering condition (30), we obtain

$$\begin{aligned}
\dot{V}_z^\star(z(t)) &\le \textstyle\sum_{i=1}^{n}\big[|z_i(t)|(-k_i|z_i(t)| + m(t))\big] \\
&+ \big[|z_n(t)|(\Gamma|\hat{z}_n(t)| + \epsilon + |o_{n-1}(t)| + k_n|o_n(t)| + |\theta(t)|)\big].
\end{aligned} \tag{31}$$

From (21), we have $|\hat{z}_n(t)| - |z_n(t)| \le |z_n(t) - \hat{z}_n(t)| = |o_n(t)|$, and describe $w(t)$ as $w(t) := \epsilon + |o_{n-1}(t)| + (k_n + 1)|o_n(t)| + |\theta(t)|$. When $R \to \infty$, $w(t) \to \epsilon$. Thus, (31) is rewritten as

$$\begin{aligned}
\dot{V}_z^\star(z(t)) &\le \textstyle\sum_{i=1}^{n}\big[|z_i(t)|(-k_i|z_i(t)| + m(t))\big] \\
&+ \big[|z_n(t)|(\Gamma|z_n(t)| + w(t))\big].
\end{aligned} \tag{32}$$

Substituting the Young's inequalities $z_i(t)m(t) \le 1/4 z_i^2(t) + m^2(t)$ and $|z_n(t)|w(t) \le 1/4 z_n^2(t) + w^2(t)$ into (32), we obtain

$$\begin{aligned}
\dot{V}_z^\star(z(t)) &\le -\textstyle\sum_{i=1}^{n}\big[(k_i - \Gamma - \frac{1}{2})z_i(t)^2\big] \\
&+ \textstyle\sum_{i=1}^{n}\big[m^2(t) + w^2(t)\big],
\end{aligned} \tag{33}$$

where $k_i - \Gamma - \frac{1}{2} > 0$. For notional brevity, let $p := 2\max_{i\in\{1,\dots,n\}}(k_i - \Gamma - 1/2)$ and $d(t) := 2n(m^2(t) + w^2(t))$. Through some simple calculations, it satisfies that

$$\dot{V}_z^\star(z(t)) = \frac{\mathrm{d}}{\mathrm{d}t}\sum_{i=1}^{n}\frac{1}{2}z_i^2(t) \le -\sum_{i=1}^{n}\frac{p}{2}z_i^2(t) + \frac{d(t)}{2}.$$

From the comparison lemma in Khalil (2002), for any $i \in \{1, \dots, n\}$, we have

$$\sum_{i=1}^{n} z_i^2(t) \le \phi(t, t_0)\sum_{i=1}^{n} z_i^2(t_0) + (1 - \phi(t, t_0))\frac{d(t)}{p}, \tag{34}$$

where $\phi(t, t_0)$ is defined as $\phi(t, t_0) := \exp(-p(t - t_0))$. When $t \to \infty$, $\phi(t, t_0) \to 0$ and $d(t) \to 2n(E^2\epsilon^2 + w^2(t))$. We define D as $D := 2n(E^2\epsilon^2 + \epsilon^2)$ and obtain

$$\limsup_{t\to\infty, R\to\infty} |z_i(t)| \le \sqrt{D/p}. \tag{35}$$

Next, we show that there is no Zeno phenomenon. From (1), (18), and (24)–(29), the following inequalities hold for $t_k \le t < t_{k+1}$,

$$\frac{\mathrm{d}}{\mathrm{d}t}\|\sigma_{1:n}(t)\| \le \|\dot{\sigma}_{1:n}(t)\| = \|\dot{x}_{1:n}(t)\|, \tag{36}$$

$$\frac{\mathrm{d}}{\mathrm{d}t}\|\dot{\tilde{\alpha}}_{n-1}(t)\| \le \|\ddot{\tilde{\alpha}}_{n-1}(t)\|, \tag{37}$$

$$\frac{\mathrm{d}}{\mathrm{d}t}|\delta_{n-1}(t)| \le |\dot{\delta}_{n-1}(t)| = |\dot{\hat{z}}_{n-1}(t)|, \tag{38}$$

$$\frac{\mathrm{d}}{\mathrm{d}t}|\delta_n(t)| \le |\dot{\delta}_n(t)| = |\dot{\hat{z}}_n(t)|. \tag{39}$$

By writing (1) and (26)–(29) in the matrix notations for $i \in \{1, \dots, n\}$, we obtain

$$\dot{x}_{1:i}(t) = A_{1:i}x_{1:i}(t) + f_{1:i}(x_{1:i}(t), t), \tag{40}$$

$$\dot{z}_{1:i}(t) = B_{1:i}z_{1:i}(t) + F_{1:i}(t), \quad t_k \le t < t_{k+1}, \tag{41}$$

where $A_{1:n} := \begin{bmatrix} 0_{(n-1)\times 1} & I_{n-1} \\ 0_{1\times 1} & 0_{1\times(n-1)} \end{bmatrix}$, $B_{1:n} := \begin{bmatrix} -k_1 & 1 & 0 & 0 & \cdots & 0 & 0 \\ -1 & -k_2 & 1 & 0 & \cdots & 0 & 0 \\ 0 & -1 & -k_3 & 1 & \cdots & 0 & 0 \\ \vdots & \vdots & \vdots & \vdots & \ddots & \vdots & \vdots \\ 0 & 0 & 0 & 0 & \cdots & -1 & -k_n \end{bmatrix}$, $z_{1:i}(t) := [z_1(t), \dots, z_i(t)]^T$, $F_{1:i}(t) := [F_1(t), \dots, F_i(t)]^T$, $F_i(t) := -\hat{f}_i(t) + f_i(x_{1:i}(t), t)$ for $i \in \{1, \dots, n-1\}$ and $F_n(t) := -\hat{f}_n(t_k) + \dot{\tilde{\alpha}}_{n-1}(t_k) - \dot{\alpha}_{n-1}(t) + f_n(x_{1:n}(t), t)$. Based on (21), we obtain $\dot{\hat{z}}_i(t) = \dot{z}_i(t) - \dot{o}_i(t)$. Then, based on state-space Eqs. (40), (41) and the uniformly ultimately bounded states, we define G as $G := \max\{A_{1:i}x_{1:i}(t) + f_{1:i}(x_{1:i}(t), t), -z_{n-2}(t) - k_{n-1}z_{n-1}(t) + z_n(t) + F_{n-1}(t) - \dot{o}_{n-1}(t), -z_{n-2}(t) - k_{n-1}z_{n-1}(t) + F_n(t) - \dot{o}_n(t), 1, \ddot{\tilde{\alpha}}_{n-1}(t)\}$. From (36)–(39) and the state transition matrix with initial conditions $\sigma_{1:n}(t_k^+) = 0$, $\delta_{n-1}(t_k^+) = 0$, $t_k^+ - t_k = 0$, $\dot{\tilde{\alpha}}_{n-1}(t_k^+) - \dot{\tilde{\alpha}}_{n-1}(t_k) = 0$ and $\delta_n(t_k^+) = 0$, we have

$$\begin{aligned}
&|\delta_{n-1}(t)| + k_n|\delta_n(t)| + L_n\|\sigma_{1:n}(t)\| + L_n|t - t_k| + |\dot{\tilde{\alpha}}_{n-1}(t) - \dot{\tilde{\alpha}}_{n-1}(t_k)| \\
&\quad \le (2 + k_n + 2L_n)\textstyle\int_{t_k^+}^{t} G\,d\tau \le (2 + k_n + 2L_n)(t - t_k)G \\
&\quad \le (2 + k_n + 2L_n)(t_{k+1} - t_k)G,
\end{aligned}$$

for some $G > 0$. Thus, there exists

$$\tau := \frac{\Gamma|z_n(t)| + \epsilon}{(2 + k_n + 2L_n)G}, \tag{42}$$

such that $|\delta_{n-1}(t)| + k_n|\delta_n(t)| + L_n\|\sigma_{1:n}(t)\| + L_n|t - t_k| + |\dot{\tilde{\alpha}}_{n-1}(t_k) - \dot{\tilde{\alpha}}_{n-1}(t)| \le \Gamma|\hat{z}_n(t)| + \epsilon$ is satisfied. This completes the proof. ■

Remark 5. In this work, the parameters λ_1, λ_2, λ_3, λ_4 and β are employed to characterize the properties of the Lyapunov functions for the ESOs, based on which the transient and steady state performance bounds of the proposed controller can be further theoretically developed. Since λ_1, λ_2, λ_3, λ_4 and β only indirectly reflect the characteristics of the ESOs and are not controller design parameters, it is challenging to evaluate the effect of these parameters on experimental results. The proposed upper bound on tracking error allows us to quantitatively analyze the impacts of these parameters on tracking performance. Specifically, from Theorem 2, we have $\limsup_{t\to\infty, R\to\infty} |z_i(t)| \le \sqrt{2n((\frac{\beta i \lambda_2 M}{\lambda_1\lambda_3})^2\epsilon^2 + \epsilon^2)/p}$, which means that the upper bound on tracking error will increase with the increase of β, λ_2, and decrease with the increase of λ_1, λ_2. In addition, as long as λ_1, λ_2, λ_3, λ_4 and β can be identified for the $g_i(\cdot)$ functions, the stability of the ESOs will be guaranteed (in the sense of bounded estimation error) and will not further affect the stability of closed-loop control, according to Theorems 1 and 2.

Remark 6. The event-triggering condition proposed in (30) guarantees the asymptotic boundedness of system states and the nonexistence of Zeno phenomenon. As shown in (30), the tradeoff between the system performance and the sampling interval can be compromised by adjusting the value of parameter ϵ, which is further analytically characterized in (35) and (42). Specifically, (35) also indicates that the stabilization of system relies on the observation error (13) and the tracking error (20). When $t \to \infty$, the observation error (13) tends to constant $E\epsilon$. and when $R \to \infty$, the tracking error (20) tends to 0.

5. Experimental results

In the literature of networked control systems, motion systems (e.g., motors) have been extensively adopted to illustrate the performance of network control algorithms (Ren, Zhang, Jiang, Yu, & Xu, 2015; Wu, She, Yu, Dong, & Zhang, 2021; Zhao, Li, & Ren, 2011; Zhou & Hu, 2015), and motor control has been a typical application of ADRC (Garrido & Luna, 2021; Wu & Huang, 2019; Ye, Bai, Zhang,

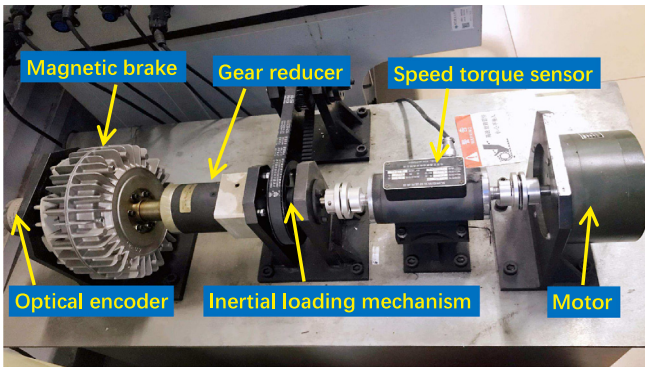

Fig. 2. Structure of the DC torque motor platform.

Qiu, & Li, 2016). To demonstrate the obtained theoretic results, we analyze the performance of the proposed controller using a DC torque motor platform (see Fig. 2) in this section. The experimental platform consists of a magnetic brake, a gear reducer, a speed torque sensor, an optical encoder, an inertial loading mechanism, a DC torque motor and a controller module that can transmit sampling and control signals. The motor considered in this work is the "130lxy" series permanent magnet DC torque motor with the maximum speed of 330 r/min, the maximum output torque of 8.25 N·m, the excitation current 11.3 A and the driving voltage of 24 V. As shown in Chen, Yao, and Wang (2013) and Huang et al. (2019), the DC motor can be described as a second-order system. To apply the proposed control approach, we note that the DC torque motor system can be modeled as

$$M\dot{v}(t) = F_{\text{ele}}(U(t)) - V_{\text{frc}}v(t) + F_{\text{fri}}(v(t)) + F_{\text{cog}}(y(t)),$$

where M denotes the inertia, $y(t)$ is the displacement, $U(t)$ is the input control signal, $F_{\text{ele}}(U(t)) := AU(t)$ denotes the electromagnetic driving force, V_{frc} denotes the viscous friction coefficient, $v(t)$ is the velocity, $F_{\text{fri}}(v(t)) := A_f \arctan(b_3 v(t))$ is the Coulomb friction, $F_{\text{cog}}(y(t)) := \sum_{i=1}^{n_f}\left(S_i \sin\left(\frac{2\pi i}{P}y(t)\right) + C_i \cos\left(\frac{2\pi i}{P}y(t)\right)\right)$ is the position dependent cogging force, and A, A_f, P, b_3, n_f, S_i, P_i are some constants based on Chen, Yao, and Wang (2013) and Xu and Yao (2001). $\dot{y}(t) = v(t) + b_1 \cos(b_2 \pi y(t))$ with constants b_1 and b_2 is also shown in Jing, Gong, Chen, Huang, and Qu (2020). The unmatched uncertainty $b_1 \cos(b_2 \pi y(t))$ is caused by the gear gap of the reducer in the motor system. Then, we define $\zeta_1(t) := y(t)$ and $\zeta_2(t) := v(t)$. The dynamics of the DC torque motor can be expressed as:

$$\begin{aligned}\dot{\zeta}_1(t) &= \zeta_2(t) + F_1(\zeta_1(t)),\\ \dot{\zeta}_2(t) &= \frac{A}{M}U(t) + F_2(\zeta_{1:2}(t)),\end{aligned}$$

where $F_1(\zeta_1(t)) := b_1 \cos(b_2 \pi \zeta_1(t))$ and $F_2(\zeta_{1:2}(t)) := -\frac{V_{\text{frc}}}{M}\zeta_2 + \frac{1}{M}F_{\text{cog}}(\zeta_1(t)) + \frac{1}{M}F_{\text{fri}}(\zeta_2)$. Since the aim is to track a pre-specified reference trajectory using the proposed event-based control approach, we define the ideal reference speed as $\zeta_2^*(t)$ and the tracking errors as $x(t) := \zeta(t) - \zeta^*(t)$. If the error system is stabilized, the tracking performance can be guaranteed. Taking $u(t) := \frac{A}{M}U(t)$, the state dynamics can be re-written as

$$\begin{aligned}\dot{x}_1(t) &= x_2(t) + f_1(x_1(t)),\\ \dot{x}_2(t) &= u(t) + f_2(x_{1:2}(t)),\end{aligned} \tag{43}$$

where $f_1(x_1(t)) := F_1(x_1(t) + \zeta_1^*(t))$ and $f_2(x_{1:2}(t)) := F_2(x(t) + \zeta^*(t)) - \dot{\zeta}_2^*(t)$.

Considering the energy restrictions in the practical applications, we restrict that the ideal reference speed $\zeta_2^*(t)$ is bounded with $\left|\zeta_2^*(t)\right| \le C_\zeta$. Let $\dot{\zeta}_1^*(t) = \zeta_2^*(t)$ and $\dot{\zeta}_2^*(t) = D(t)$, where $D(t)$ denotes the designed function satisfying $|D(t)| + |\dot{D}(t)| \le C_D$ for some $C_D > 0$. Since uncertainties f_1 and f_2 are simple combinations of $\sin(\cdot)$, $\cos(\cdot)$ and $\arctan(\cdot)$ functions which are bounded, Assumptions 1–3 are satisfied. To verify

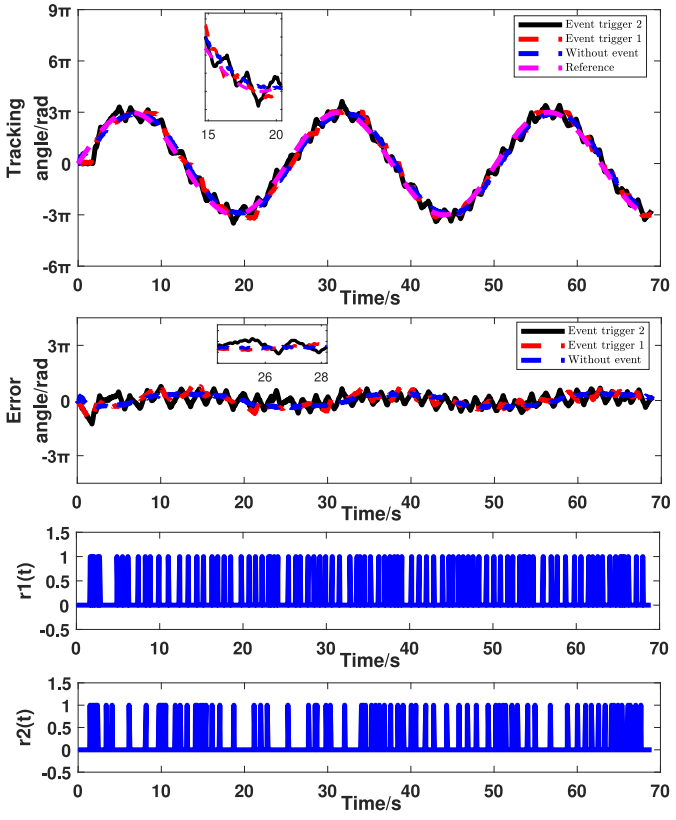

Fig. 3. Tracking performance comparison for a sine-wave reference signal.

Assumption 4, we define Hurwitz matrixes N_1 and N_2 as $\begin{bmatrix}-2 & 1\\ -1 & 0\end{bmatrix}$ and $\begin{bmatrix}-2 & 1 & 0 & 0\\ -1 & 0 & 0 & 0\\ -2 & 0 & -2 & 1\\ -1 & 0 & -1 & 0\end{bmatrix}$, respectively. Then matrixes $P_1 = \begin{bmatrix}0.5 & -0.5\\ -0.5 & 1.5\end{bmatrix}$ and $P_2 = \begin{bmatrix}11/16 & -5/16 & -1/8 & -1/8\\ -11/16 & 23/16 & 1/8 & -3/8\\ -1/8 & 1/8 & 1/2 & -1/2\\ -1/8 & -3/8 & -1/2 & 3/2\end{bmatrix}$ are obtained by solving $P_i N_i + N_i^T P_i = -I$ for $i \in \{1,2\}$, where I is an identity matrix. Thus we have $\lambda_{\min}(P_i)\|e^i\|^2 \le \langle P_i e^i, e^i\rangle \le \lambda_{\max}(P_i)\|e^i\|^2$. Define $V_i(e^i)$ as $V_i(e^i) := \langle P_i e^i, e^i\rangle$, and we have $\lambda_{\min}(P_i)\|e^i\|^2 \le V_i(e^i) \le \lambda_{\max}(P_i)\|e^i\|^2$, $\sum_{j=1}^{2}(\frac{\partial V_i}{\partial e_j}(e_{2+j} - g_j(e_1 + \cdots + e_j)) - \frac{\partial V_i}{\partial e_{2+j}}(g_{2+j}(e_1 + \cdots + e_j))) \le -\|e^i\|^2$, and $\left\|\frac{\partial V_i}{\partial e^i}\right\| \le \|2e^{iT}P_i\| \le 2\lambda_{max}(P_i)\|e^i\|$. Then, by taking $\lambda_1 = \min\left\{\lambda_{\min}(P_1), \lambda_{\min}(P_2)\right\} = 0.2929$, $\lambda_2 = \max\left\{\lambda_{\max}(P_1), \lambda_{\max}(P_2)\right\} = 2.0274$, $\lambda_3 = 1$, $\lambda_4 = 1$ and $\beta = 2 \cdot \lambda_2 = 4.0548$, Assumption 4 is satisfied.

To implement the proposed controller, we define the extended state as $x_{n+i}(t) := f_i(x_{1:i}(t), t)$ and design $q_i = 1$ for $i = 1, 2, 3, 4$, the high-gain parameter as $\varepsilon = 0.2$, and the observer functions as $g_i(z) = 2z$, $g_{n+i}(z) = z$ to construct the ESOs in (2). As a result, the bank of ESOs have the following form:

$$\begin{aligned}\dot{\hat{x}}_1(t) &= x_2(t) + \hat{x}_3(t) + \frac{2}{\varepsilon}(x_1(t) - \hat{x}_1(t)),\\ \dot{\hat{x}}_3(t) &= \frac{1}{\varepsilon}(x_1(t) - \hat{x}_1(t)),\\ \dot{\hat{x}}_2(t) &= u(t) + \hat{x}_4(t) + \frac{2}{\varepsilon}(x_1(t) - \hat{x}_1(t) + x_2(t) - \hat{x}_2(t)),\\ \dot{\hat{x}}_4(t) &= \frac{1}{\varepsilon}(x_1(t) - \hat{x}_1(t) + x_2(t) - \hat{x}_2(t)).\end{aligned}$$

Note that the number of ESOs designed is equal to the order of the system (which is two in this example). Then, the controller is designed as $u(t) := -\tilde{z}_1(t_k) - 5\tilde{z}_2(t_k) - \hat{f}_2(t_k) + \dot{\hat{\alpha}}_1(t_k)$. In this work, we choose two different kinds of reference trajectory inputs, which are sine-wave input and squarewave input, to carry out the experiments. These signals are typical testing signals used in motion control systems for performance evaluation (Bifaretti, Tomei, & Verrelli, 2011; Huang

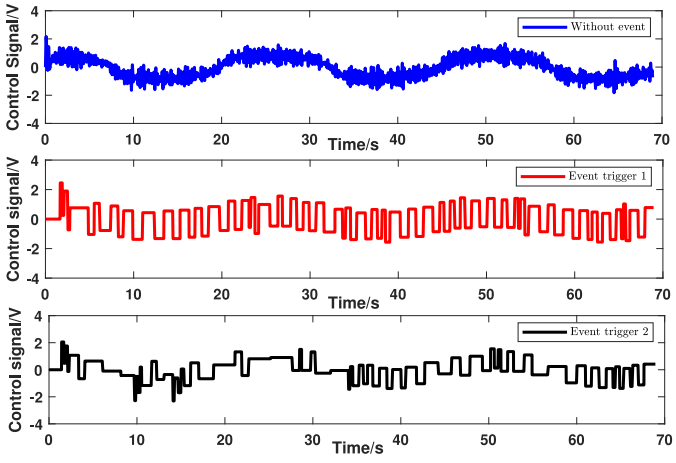

Fig. 4. Control signals for a sine-wave reference signal.

Table 1
Performance metrics of sine-wave tracking.

Controller setting	ϵ	Tracking errors	RMSEs	Average sample time
Without trigger	–	0.77 rad	0.86 rad	–
Event trigger 1	6	0.80 rad	0.96 rad	382 ms
Event trigger 2	8	0.86 rad	1.08 rad	441 ms

et al., 2019; Lee & Youn, 2004; Verrelli, Tomei, & Lorenzani, 2018). In particular, the sine-wave signals are normally utilized to test the dynamic tracking performance of the system, while the square-wave signals tend to approximate the step signals and can be used to test the static performance. In order to evaluate the tracking performance of the event-triggered system, we define the tracking errors as the ratio between the integral of absolute tracking errors and the total experiment time, and the average sampling time as the ratio between total experimental time and total triggering numbers, respectively. Moreover, the root-mean-square errors (RMSEs) are evaluated to show the dispersion of the tracking errors.

Firstly, we consider the scenario of sine-wave reference signals. The results and the output of the event-triggering condition are shown in Fig. 3; the control signals are shown in Fig. 4; the tracking errors and the average sample time are summarized in Table 1. In particular, only when $r(t) = 1$ will the measurement updates be transmitted. Note that the aim of the proposed event-triggered controller is not to achieve improved performance compared with time-triggered control, but to maintain similar performance at reduced controller update rate. Specifically, as is shown in Fig. 3, when the sampling frequency is high ($\epsilon = 6$), the controller with event trigger 1 achieves a tracking error around 0.8 rad, which is almost the same as that of the time-triggered controller (0.77 rad). The controller update frequency is further reduced by event trigger 2, but the tracking performance is not significantly decreased. Moreover, we note that for the proposed event-triggered control approach, the control signal is only updated when the event-triggering condition is violated. Since the proposed event-triggering condition is basically designed based on real-time tracking error, the consequence is that the actual tracking error response will fluctuate around zero (partially also due to the existence of external disturbances).

The observations in the scenario of squarewave reference signals is also considered using the proposed event-triggered backstepping controller, the results of which are shown in Figs. 5, 6 and Table 2, which are consistent with those for the case of sine-wave reference signals. In general, we observe that the event-triggered backstepping controller provides an efficient way to maintain the system performance by reducing communication rate, which is particularly useful to practical applications with limited energy and communication resources.

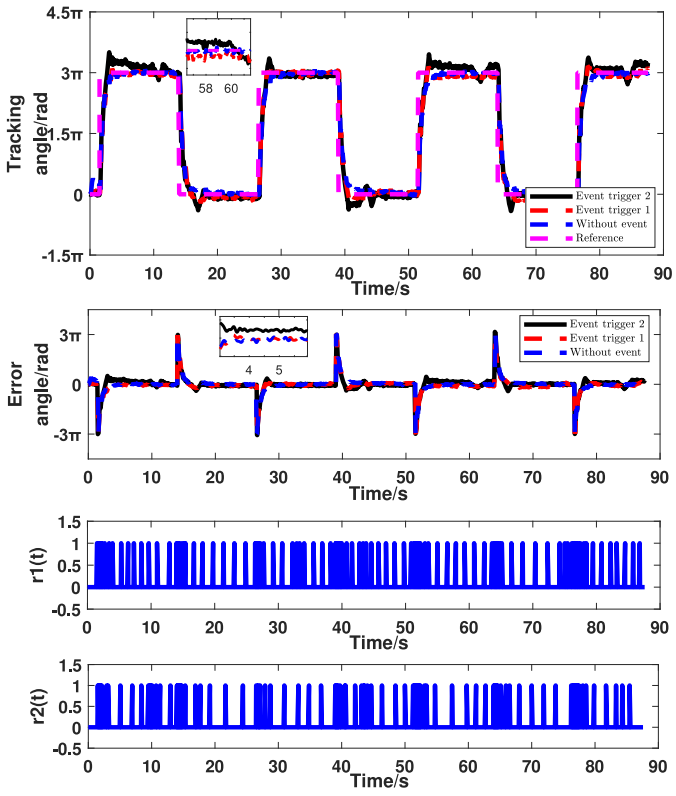

Fig. 5. Tracking performance comparison for a squarewave reference signal.

Table 2
Performance metrics of squarewave tracking.

Controller setting	ϵ	Tracking errors	RMSEs	Average sample time
Without trigger	–	0.55 rad	1.47 rad	–
Event trigger 1	6	0.59 rad	1.48 rad	236 ms
Event trigger 2	8	0.64 rad	1.52 rad	263 ms

6. Conclusion and future work

In this work, a stabilization problem for event-triggered systems with control-unmatched uncertainties is investigated. A bank of ESOs is proposed to estimate the n-dimensional uncertainties, and a Zeno-free event-triggering condition is designed to reduce communication rate while guaranteeing closed-loop stability. The performance of the event-triggered controller is validated through experimental results on a DC torque motor platform for different reference signals and different event-triggered schedules. In our current study, the state feedback information is available, and the output feedback control scenario will be investigated in our future work.

Declaration of competing interest

The authors declare that they have no known competing financial interests or personal relationships that could have appeared to influence the work reported in this paper.

Acknowledgments

The authors would like to thank the Associate Editor and the anonymous reviewers for their suggestions which have improved the quality of the work.

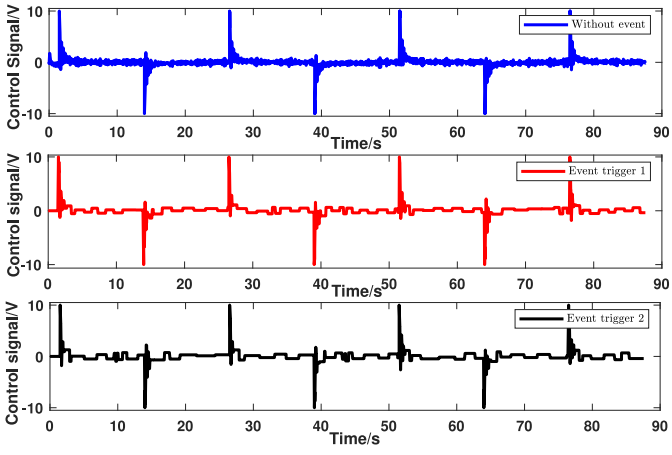

Fig. 6. Control signals for a squarewave reference signal.

References

Åarzén, K.-E. (1999). A simple event-based PID controller. *IFAC Proceedings Volumes*, *32*(2), 8687–8692.

Bifaretti, S., Tomei, P., & Verrelli, C. M. (2011). A global robust iterative learning position control for current-fed permanent magnet step motors. *Automatica*, *47*(1), 227–234.

Borgers, D. P., Dolk, V. S., & Heemels, W. P. M. H. (2018). Riccati-based design of event-triggered controllers for linear systems with delays. *IEEE Transactions on Automatic Control*, *63*(1), 174–188.

Brunner, F. D., Heemels, W., & Allgöwer, F. (2019). Event-triggered and self-triggered control for linear systems based on reachable sets. *Automatica*, *101*, 15–26.

Chen, S., Xue, W., & Huang, Y. (2019). Analytical design of active disturbance rejection control for nonlinear uncertain systems with delay. *Control Engineering Practice*, *84*, 323–336.

Chen, Z., Yao, B., & Wang, Q. (2013). Adaptive robust precision motion control of linear motors with integrated compensation of nonlinearities and bearing flexible modes. *IEEE Transactions on Industrial Informatics*, *9*(2), 965–973.

Chen, Z., Yao, B., & Wang, Q. (2013). Adaptive robust precision motion control of linear motors with integrated compensation of nonlinearities and bearing flexible modes. *IEEE Transactions on Industrial Informatics*, *9*(2), 965–973.

Feng, H., & Guo, B. (2017). A new active disturbance rejection control to output feedback stabilization for a one-dimensional anti-stable wave equation with disturbance. *IEEE Transactions on Automatic Control*, *62*(8), 3774–3787.

Forni, F., Galeani, S., Nesic, D., & Zaccarian, L. (2014). Event-triggered transmission for linear control over communication channels. *Automatica*, *50*(2), 490–498.

Garrido, R., & Luna, L. (2021). Robust ultra-precision motion control of linear ultrasonic motors: A combined ADRC-luenberger observer approach. *Control Engineering Practice*, *111*, Article 104812.

Guo, B., & Han, J. (2000). A linear tracking-differentiator and application to the online estimation of the frequency of a sinusoidal signal. In *IEEE international conference on control applications* (pp. 9–13).

Guo, B., & Wu, Z. (2017). Output tracking for a class of nonlinear systems with mismatched uncertainties by active disturbance rejection control. *Systems & Control Letters*, *100*, 21–31.

Guo, B., & Zhao, Z. (2011). On convergence of tracking differentiator and application to frequency estimation of sinusoidal signals. In *2011 8th Asian control conference* (pp. 1470–1475).

Guo, B., & Zhao, Z. (2011). On convergence of tracking differentiator. *International Journal of Control*, *84*(4), 693–701.

Han, D., Mo, Y., Wu, J., Weerakkody, S., Sinopoli, B., & Shi, L. (2015). Stochastic event-triggered sensor schedule for remote state estimation. *IEEE Transactions on Automatic Control*, *60*(10), 2661–2675.

He, X., Hu, C., Xue, W., & Fang, H. (2017). On event-based distributed Kalman filter with information matrix triggers. *IFAC-PapersOnLine*, *50*(1), 14308–14313.

Huang, Y., Wang, J., Shi, D., & Shi, L. (2018). Toward event-triggered extended state observer. *IEEE Transactions on Automatic Control*, *63*(6), 1842–1849.

Huang, Y., Wang, J., Shi, D., Wu, J., & Shi, L. (2019). Event-triggered sampled-data control: An active disturbance rejection approach. *IEEE/ASME Transactions on Mechatronics*, *24*(5), 2052–2063.

Jing, L., Gong, J., Chen, J., Huang, Z., & Qu, R. (2020). A novel coaxial magnetic gear with unequal halbach arrays and non-uniform air gap. *IEEE Transactions on Applied Superconductivity*, *30*(4), 1–5.

Khalil, H. K. (2002). Nonlinear systems. In *Prentice-Hall*.

Kim, D. S., Choi, D. H., & Mohapatra, P. (2009). Real-time scheduling method for networked discrete control systems. *Control Engineering Practice*, *17*(5), 564–570.

Kung, E., Wang, J., Wu, J., Shi, D., & Shi, L. (2019). On the nonexistence of event triggers that preserve Gaussian state in presence of packet-drop. *IEEE Transactions on Automatic Control*, 1.

Lee, J. H., & Youn, M. J. (2004). A new improved continuous variable structure controller for accurately prescribed tracking control of BLDD servo motors. *Automatica*, *40*(12), 2069–2074.

Li, Y., & Yang, G. (2018). Event-triggered adaptive backstepping control for parametric strict-feedback nonlinear systems. *International Journal of Robust and Nonlinear Control*, *28*(3), 976–1000.

Li, W., Zhang, X., & Li, H. (2014). Co-simulation platforms for co-design of networked control systems: An overview. *Control Engineering Practice*, *23*, 44–56.

Li, S., Zhu, C., Mao, Q., Su, J., & Li, J. (2021). Active disturbance rejection vibration control for an all-clamped piezoelectric plate with delay. *Control Engineering Practice*, *108*, Article 104719.

Liang, C., Ge, M., Liu, Z., Ling, G., & Liu, F. (2021). Predefined-time formation tracking control of networked marine surface vehicles. *Control Engineering Practice*, *107*, Article 104682.

Liu, L., Li, X., Liu, Y., & Tong, S. (2021). Neural network based adaptive event trigger control for a class of electromagnetic suspension systems. *Control Engineering Practice*, *106*, Article 104675.

Liu, C., Li, H., & Shi, Y. (2020). Resource-aware exact decentralized optimization using event-triggered broadcasting. *IEEE Transactions on Automatic Control*, 1.

Liu, C., Li, H., Shi, Y., & Xu, D. (2020a). Codesign of event trigger and feedback policy in robust model predictive control. *IEEE Transactions on Automatic Control*, *65*(1), 302–309.

Liu, C., Li, H., Shi, Y., & Xu, D. (2020b). Distributed event-triggered gradient method for constrained convex minimization. *IEEE Transactions on Automatic Control*, *65*(2), 778–785.

Liu, D., Wang, J., Wang, S., & Shi, D. (2020). Active disturbance rejection control for electric cylinders with PD-type event-triggering condition. *Control Engineering Practice*, *100*, Article 104448.

Lu, C., Wu, M., Chen, L., & Cao, W. (2021). An event-triggered approach to torsional vibration control of drill-string system using measurement-while-drilling data. *Control Engineering Practice*, *106*, Article 104668.

Madonski, R., Stanković, M., Shao, S., Gao, Z., Yang, J., & Li, S. (2020). Active disturbance rejection control of torsional plant with unknown frequency harmonic disturbance. *Control Engineering Practice*, *100*, Article 104413.

Postoyan, R., Sanfelice, R. G., & Heemels, W. P. M. H. (2019). Inter-event times analysis for planar linear event-triggered controlled systems. In *2019 IEEE 58th conference on decision and control* (pp. 1662–1667).

Rathore, N., Fulwani, D., & Rathore, A. K. (2020). Event-triggered sliding mode control for light load efficiency improvement in power converters. *Control Engineering Practice*, *100*, Article 104429.

Ren, M., Zhang, J., Jiang, M., Yu, M., & Xu, J. (2015). Minimum (h, ϕ)– entropy control for non-Gaussian stochastic networked control systems and its application to a networked DC motor control system. *IEEE Transactions on Control Systems Technology*, *23*(1), 406–411.

Sahoo, A., Xu, H., & Jagannathan, S. (2013). Neural network-based adaptive event-triggered control of nonlinear continuous-time systems. In *IEEE international symposium on intelligent control* (pp. 35–40).

Sahoo, A., Xu, H., & Jagannathan, S. (2013). Neural network-based adaptive event-triggered control of nonlinear continuous-time systems. In *IEEE international symposium on intelligent control* (pp. 35–40).

Shi, D., Chen, T., & Darouach, M. (2016). Event-based state estimation of linear dynamic systems with unknown exogenous inputs. *Automatica*, *69*, 275–288.

Tabuada, P. (2007). Event-triggered real-time scheduling of stabilizing control tasks. *IEEE Transactions on Automatic Control*, *52*(9), 1680–1685.

Trimpe, S., & D'Andrea, R. (2014a). Event-based state estimation with variance-based triggering. *IEEE Transactions on Automatic Control*, *59*(12), 3266–3281.

Trimpe, S., & D'Andrea, R. (2014b). Event-based state estimation with variance-based triggering. *IEEE Transactions on Automatic Control*, *59*(12), 3266–3281.

Verrelli, C. M., Tomei, P., & Lorenzani, E. (2018). Persistency of excitation and position-sensorless control of permanent magnet synchronous motors. *Automatica*, *95*, 328–335.

Wang, W., Postoyan, R., Nešić, D., & Heemels, W. P. M. H. (2020). Periodic event-triggered control for nonlinear networked control systems. *IEEE Transactions on Automatic Control*, *65*(2), 620–635.

Wei, W., Xue, W., & Li, D. (2019). On disturbance rejection in magnetic levitation. *Control Engineering Practice*, *82*, 24–35.

Wu, Z., Deng, F., Guo, B., C, & Xiang, Q. (2021). Backstepping active disturbance rejection control for lower triangular nonlinear systems with mismatched stochastic disturbances. *IEEE Transactions on Systems, Man, and Cybernetics: Systems*, 1–15.

Wu, H., & Huang, J. (2019). Control of induction motor drive based on ADRC and inertia estimation. In *2019 IEEE international electric machines drives conference* (pp. 1607–1612).

Wu, X., She, J., Yu, L., Dong, H., & Zhang, W. (2021). Contour tracking control of networked motion control system using improved equivalent-input-disturbance approach. *IEEE Transactions on Industrial Electronics*, *68*(6), 5155–5165.

Wu, X., & Xie, L. (2019). Performance evaluation of industrial Ethernet protocols for networked control application. *Control Engineering Practice*, *84*, 208–217.

Xu, L., & Yao, B. (2001). Adaptive robust precision motion control of linear motors with negligible electrical dynamics: theory and experiments. *IEEE/ASME Transactions on Mechatronics*, *6*(4), 444–452.

Xue, W., & Huang, Y. (2014). On performance analysis of ADRC for a class of MIMO lower-triangular nonlinear uncertain systems. *ISA Transactions*, *53*(4), 955–962.

Xue, W., Huang, Y., & Gao, Z. (2016). On ADRC for non-minimum phase systems: canonical form selection and stability conditions. *Control Theory and Technology*, *14*(3), 199–208.

Xue, W., Madonski, R., Lakomy, K., Gao, Z., & Huang, Y. (2017). Add-on module of active disturbance rejection for set-point tracking of motion control systems. *IEEE Transactions on Industry Applications*, *53*(4), 4028–4040.

Ye, Y., Bai, M., Zhang, Z., Qiu, W., & Li, R. (2016). A design of dredger cutter motor synchronous speed control system based on ADRC. In *2016 Chinese control and decision conference* (pp. 1646–1650).

Zhang, D., Ye, Z., Chen, P., & Wang, Q. (2020). Intelligent event-based output feedback control with Q-learning for unmanned marine vehicle systems. *Control Engineering Practice*, *105*, Article 104616.

Zhao, Z., & Guo, B. (2015). Extended state observer for uncertain lower triangular nonlinear systems. *Systems & Control Letters*, *85*, 100–108.

Zhao, Z., & Guo, B. (2018). A novel extended state observer for output tracking of MIMO systems with mismatched uncertainty. *IEEE Transactions on Automatic Control*, *63*(1), 211–218.

Zhao, D., Li, C., & Ren, J. (2011). Fuzzy speed control and stability analysis of a networked induction motor system with time delays and packet dropouts. *Nonlinear Analysis. Real World Applications*, *12*(1), 273–287.

Zhou, Y., & Hu, S. (2015). H infinity control for DC servo motor in the network environment. In *2015 IEEE Advanced information technology, electronic and automation control conference* (pp. 401–405).